Colloid Polym Sci (2002) 280: 956–962
DOI 10.1007/s00396-002-0714-z

ORIGINAL CONTRIBUTION

Szilvia Papp
Imre Dékány

Growth of Pd nanoparticles on layer silicates hydrophobized with alkyl chains in ethanol-tetrahydrofuran mixtures

Received: 20 February 2002
Accepted: 8 April 2002

S. Papp · I. Dékány (✉)
Nanostructured Materials Research
Group of the Hungarian Academy
of Science 6720 Szeged, Hungary
E-mail: i.dekany@chem.u-szeged.hu
Tel.: +36-62-544211
Fax: +36-62-544042

I. Dékány
Department of Colloid Chemistry
University of Szeged,
Aradi Vértanúk tere 1,
6720 Szeged, Hungary

Abstract The surface of montmorillonite, a hydrophilic layer silicate, was modified with alkylammonium and alkylpyridinium cations with the aim of producing Pd nanoparticles within the hydrophobized interlamellar space. The structure and interlamellar swelling of hexadecylpyridinium and tetradodecylammonium montmorillonite were first studied in tetrahydrofuran-ethanol mixtures. It was established that both hydrophobic montmorillonites swell readily in tetrahydrofuran and the interlamellar spaces may be employed as nanoreactors for the synthesis of Pd^o particles. Ethanol was adsorbed on the surface of the hydrophobic support. After addition of the precursor Pd-acetate, metallic Pd was produced on the external and internal surfaces of the support. The diameter of the particles formed was in the range of 2–5 nm as shown by TEM.

Introduction

Several methods have been described for the preparation of various semiconductor and transition metal nanoparticles. [1, 2]. The preparations utilizing polymers, association colloids (micelles), microemulsions, Langmuir-Blodgett (LB) films [3], or other self-assembling systems (SA) have been discussed in detail in the literature [4] in relation to the stabilization of particles and the control of particle size. These methods include reactions performed in both organic and aqueous mediums. Stabilizing agents protecting the newly formed nanoparticles against aggregation play an important role in these procedures. Their use makes feasible the generation of very small particles, with diameters of a few nanometers. The most commonly used stabilizers are polymers [5, 6, 7, 8, 9, 10], alkylammonium salts [11, 12], and surfactants [13, 14, 15]. Colloid particles of controlled size were also prepared within the internal space of micelles [16, 17] and microemulsions [18].

In our earlier studies, the adsorption layer at the solid/liquid interface was utilized as a nanophase reactor for the preparation of nanocrystalline semiconductors (CdS, ZnS, TiO_2) and for their stabilization [19, 20]. CdS and ZnS nanoparticles were prepared on the surface of spherical silica supports (Aerosil 200) and minerals of layered structure (hydrophobized montmorillonite, pillared montmorillonite, double layer hydroxides) [21, 22, 23]. The main point of the procedure is to adsorb the precursor ions in the adsorption layer on the surface of the solid particles (i.e. clay mineral lamellae) dispersed in a liquid medium and to carry out the synthesis within the surface layer by delivering the appropriate reducing agent (alcohols, hydrazine, borohidride etc.) to this layer. A composition of the dispersion medium is selected in which the precursor ions are practically insoluble. When the solubility in the liquid phase is poor, precursor ions are preferentially adsorbed on the solid surface and their concentration within the bulk phase is close to zero. When a reducing agent is added to a system that has attained adsorption equilibrium, particles will be formed only in the surfacial adsorption layer and grow to nanocrystals attached to the surface. Their size and number can then be easily controlled [22, 24]. This controlled colloid synthesis is basically different from the impregnation technique used for the preparation of metal catalysts. Clay minerals (montmorillonite, hectorite, saponite etc.) are suitable for this purpose because they swell readily in aqueous medium and provide a large internal surface [25]. The silicate lamellae are negatively charged and their surface is covered by charge-compensating cations (e.g. Na^+, Ca^{2+}) that can be exchanged for the precious metal cations such as Pd cations, which are reducing, by agents like alcohol or hydrazine.

Preparation of Pd nanoparticles via ethanol reduction of Pd acetate in organic suspensions of hydrophobized montmorillonite was reported by Király and coworkers [26]. Montmorillonite modified by alkylammonium or alkylpyridinium cations was first swollen in toluene, then Pd acetate (a salt extensively soluble in the organic medium) was adsorbed in the interlamellar space and reduced by ethanol at room temperature. Using a similar procedure, Pd^{2+} ions were adsorbed on pillared montmorillonite and then Pd nanoparticles of 4–10 nm diameter were prepared by reduction [27].

In our previous publication, we described the production of Pd^{o} nanoparticles stabilized by a cationic surfactant (tetradodecylammonium bromide). In the present work, alkyl chains promoting stabilization are immobilized on the surface of layered structure and Pd nanoparticles are generated in situ within the hydrophobic interlamellar space. Thus, instead of preparation within droplets of microemulsions (serving as nanoreactors), the role of stabilization is assigned to the clay mineral swollen in organic medium. One of the advantages of this method is the immobilization of the nanoparticles at the supporting clay mineral.

Materials and methods

Materials

The following materials were used for the experiments: tetrahydrofurane (THF, C_4H_8O, 99,8%, Carlo Erba), ethanol (EtOH, C_2H_6O, 99.8%, Reanal), palladium acetate (Pd $(OAc)_2$, $C_4H_6O_4Pd$, 99%, Merck), tetradodecylammonium bromide (TDOABr, $C_{48}H_{100}BrN$, 99%, Fluka), hexadecylpyridinium chloride (HDPCl, $C_{21}H_{38}ClN$, 98%, Fluka).

Preparation of hydrophobic montmorillonites

The hydrophobized montmorillonites were prepared by cation exchange of Na-montmorillonite. The Na-montmorillonite for the derivatization with hexadecylpyridinium (HDP^+) cations was prepared from bentonite from Mád (Northern Hungary, Tokaj Mountain) by peptization with $NaCO_3$. The fine fraction (diameter d ≤ 2 μm) was separated by sedimentation and the suspension was stirred with 1 M NaCl solution. The dispersion was washed in distilled water and centrifuged several times, evaporated, dried, ground, and passed through a 60 mesh sieve. The purity of the Na-montmorillonite was checked by X-ray powder diffraction. The cation exchange capacity (c.e.c.) of the sample was 0.89 meq/g montmorillonite (NH_4 acetate method).

Tetradodecylammonium ($TDOA^+$) montmorillonite was obtained by organophilization of Schwaiba montmorillonite (SÜDCHEMIE A.G., Germany). The c.e.c. value of this Na-montmorillonite was 0.85 meq/g montmorillonite. The fine fraction (d ≤ 2 μm) was obtained by peptization with $NaCO_3$.

The surfactant solutions for the exchange reactions were 1% HDPCl solution in water and 0.2% TDOABr solution in ethanol/water mixture (1:1). An amount 1.5 times the c.e.c. value was added to a 1% suspension of Na-montmorillonite, which was coagulated by the hydrophobizing effect of the surfactant. The hydrophobic organoclay complex was filtered, washed in ethanol/water mixture (1:1), dried at 60°C, ground, and passed through a 60 mesh sieve. The incorporation of the alkyl ammonium ions in the interlamellar space was checked by X-ray powder diffraction.

Synthesis of Pd^{o} particles

Hydrophobic montmorillonites [HDP-montmorillonite; TDOA-montmorillonite 50% c.e.c. (sample I); 100% c.e.c. (sample II)] were dispersed in THF at 63% (w/v) concentration. Ethanol was added to produce compositions corresponding to volume fractions of $x_1 = 0.005$, 0.01, and 0.02. Ethanol adsorption increases the interlamellar expansion of the organophilic montmorillonite but also reduces the Pd^{2+} ions. Pd-acetate (0.1, 0.15, or 0.20 mmol/1 g organoclay) dissolved in THF was next added to the dispersion, which was stirred on a magnetic stirrer. Reduction was indicated by the darkening color of the suspension. At higher $Pd(OAc)_2$ concentrations the dispersion turned black after stirring for 24 h. The metal content of the dispersion with respect to the support was 1.06, 1.6, and 2.12% (w/w), respectively. The scheme of the synthesis is shown in Fig. 1.

Methods

X-ray powder diffraction

X-ray diffraction measurements were taken on a Philips PW 1820 diffractometer, CuK_α radiation ($\lambda = 0.154$ nm), 40 kV, 35 mA, $1^0 \leq 2\Theta \leq 50^0$. The basal spacing d_L was calculated from the first (001) Bragg reflection by using the PW 1877 automated powder diffraction software.

The mean diameter, D, of crystallites is related to the X-ray diffraction broadening, β, by the Scherrer equation: $D = k\alpha/\beta \cos\Theta$, where k is approximate (varying between 0.79 and 1.7) and related to the crystallite shape and to the way in which β and D are defined. The radiation wavelength is α and the Bragg angle Θ. β must be carefully distinguished from the breadth of diffraction line (B) as actually observed under given experimental conditions, $\beta = (B^2 - b^2)^{1/2}$ [28].

Electron microscopy

Transmission electron microscopy (TEM) is suitable for the examination of colloids since its range of measurement covers particles of size 1–50 nm. Images were made in a Philips CM-10 transmission electron microscope with an accelerating voltage of 100 kV. Aliquots of ethanol dispersions of the samples were dropped onto copper grids (diameter 2 mm) covered with Formwar foil, left to stand for 3–40 s, and transferred into the microscope. The particle size distribution was determined by using the UTS-HCSA Image Tool program.

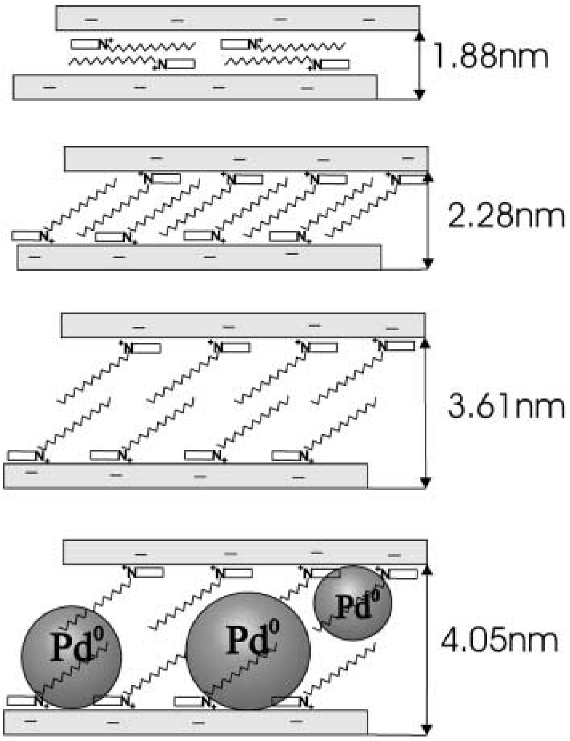

Fig. 1. Interlamellar structure of HDP montmorillonite (**a**) bilayer of parallel chains (**b**) expansion to a distance equal the length of the alkyl chain (**c**) expansion to twice the length of the alkyl chain (totally expanded state) (**d**) HDP-montmorillonite stabilized Pd^0

Results and discussion

The structure of montmorillonites organophilized with hexadecylpyridinium chloride has been known since the nineteen-seventies from the works of Weiss, Stange, and Lagaly [29, 30, 31, 32, 33]. In the present discussion, measurement of the basal spacing in THF suspension gains special importance because the precursor ions can not only be bound on the external but also on the internal surface of the mineral, i.e. in the interlamellar space. The scheme shown in Fig. 1 is based on XRD measurements. The basal spacing of the dry sample is $d_L = 1.87$ nm, a value corresponding to parallel bilayers (Fig. 1a). HDP-montmorillonite swells readily in THF and d_L increases to 3.98 nm, i.e. the layers move apart and the bilayer contains tilted alkyl chains with a tilting angle of 35° (Fig. 1b, c). The basal spacing calculated for $n_c = 16$ is $d_L = 0.96 + [(n_c \times 0.127 + 0.28)\sin 35°] = 2.28$ nm when expansion proceeds to a distance that equals the length of the alkyl chain (Fig. 1b) and $d_L = 3.61$ when expansion proceeds to twice the length of the alkyl chain (Fig. 1c, totally expanded state). (The average cross-sectional area of straight-chain alkyl chains is 0.205 nm^2 and the length of the terminal methyl group is 0.28 nm). Comparison with the experimental data reveals that the latter structure is realized. Knowing the experimental value for d_L, the free interlamellar volume available as a "nanoreactor" for the particle growth is calculated. The interlamellar volume is $V_{int} = 0.232(d_L – 0.96)$ nm^3/$(SiAl)O_4$ formula unit. The volume of the HDP molecule is $V_{alk} = [(n_c \times 0.127 + 0.28) \times 0.205] + 0.12$ nm^3 (where 0.12 nm^3 is the approximate volume of the pyridinium ring). Taking into account the layer charge ($\zeta = 0.32$ for montmorillonite), the liquid volume V_f relative to one formula unit of $(SiAl)_4O_{10}$ is calculated from $V_f = V_{int} – \zeta V_{alk}$. Based on d_L, the observed values for HDP montmorillonite V_f is 0.507 nm^3/formula unit in THF and 0.401 nm^3/formula unit in ethanol. The basal spacing in THF/ethanol mixtures containing small amounts of ethanol ($x_1 = 0.005$, 0.01, and 0.02) were 4.08, 4.25, and 4.39 nm, respectively. Thus, the interlamellar expansion was further enhanced in THF/ethanol mixtures and V_f is increased to 0.534, 0.574, and 0.601 $nm^3/(SiAl)_4O_{10}$ unit, respectively. The importance of this swelling effect is stressed by the fact that it lies in the composition range where $Pd(OAc)_2$ is reduced in the interfacial layer. Higher ethanol concentrations were not tested. If the ethanol concentration is increased, reduction already takes place also in the bulk phase which leads to the formation of microcrystalline Pd^o particles in the dispersion.

Based on our earlier liquid sorption experiments, it was established that ethanol is preferentially adsorbed in the surfacial layer at low ethanol concentrations ($x_1 = 0.005–0.02$), i.e. the composition in the interlamellar space (the nanoreactor) corresponds to molar fractions $x_1{}^s = 0.6–0.8$. Thus, for the reduction of Pd^{2+} ions in the adsorption layer, the reducing agent concentrations are high ($c_0 = 0.002–0.004$ mmol/l, $c_{V_s} = 0.1–0.2$ mmol/l), ensuring that nanoparticles are formed only in the interlamellar volume V_f, a circumstance that supports helps stabilization of the nanoparticles.

When the cationic surfactant with four alkyl chains is used for hydrophobization, d_L is considerably larger due to steric reasons. At 50% cation exchange, the alkyl chains still have enough room for a bilayer orientation between the layers (Fig. 2a), corresponding to an interlamellar distance of $d_L = 4 \times 0.46 + 0.96$ ($= 2.8$ nm). The expanded spacing of the dried sample in good agreement is $d_L = 2.91$ nm. Dry TDOA-montmorillonite II prepared at 100% cation exchange appears to have a similar orientation of the surfactant molecules ($d_L = 3.12$ nm). When this sample is swollen in THF, the d_L value becomes characteristic of a bilayer structure with perpendicular chain orientation ($d_L = 4.13$ nm), in good agreement with the calculated value, $d_L = 2 \times (n_c \times 0.127 + 0.28) + 0.96 = 4.36$ (Fig. 2b). Again, these d_L values can be used for calculation of the free interlamellar volume $V_f = V_{int} – \zeta V_{alk}$ which is 0.356 nm^3 for TDOA-montmorillonite (50% exchange) and

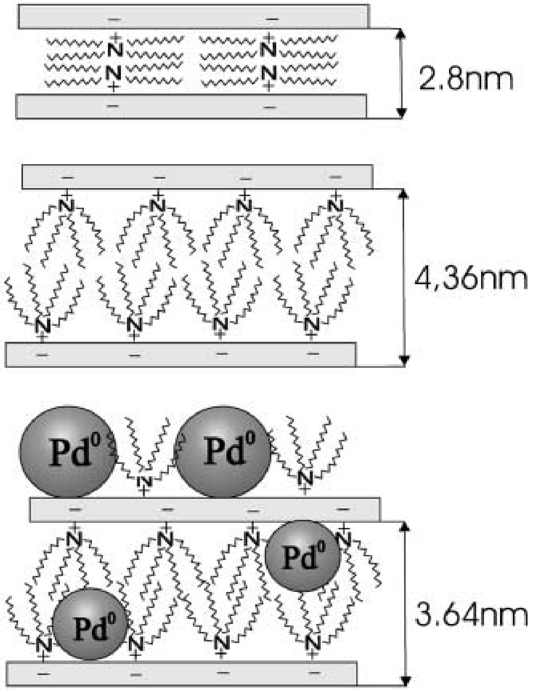

Fig. 2. Interlamellar structure of TDOA montmorillonite (**a**) 2 × 2 bilayer structure (**b**) bilayer structure with perpendicular chain orientation (**c**) TDOA-montmorillonite stabilized Pd^0 nanoparticles

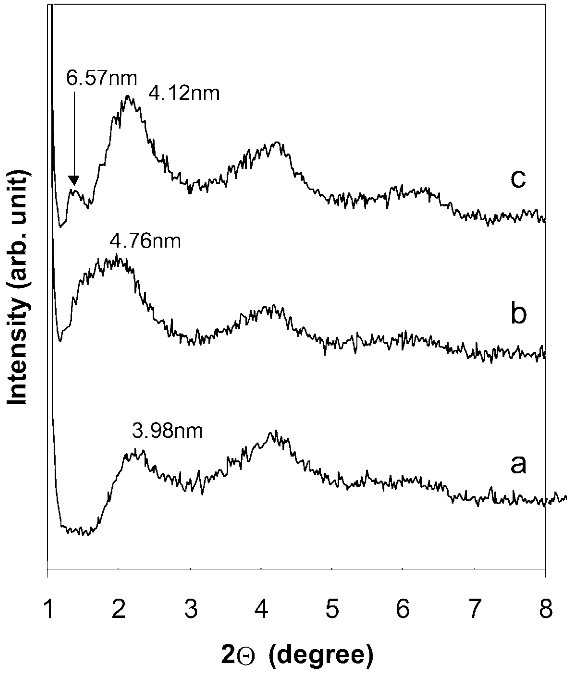

Fig. 3. XRD patterns of (**a**) HDP-montmorillonite swollen in THF (**b**) HDP-montmorillonite with 1.6% Pd in suspension (**c**) HDP-montmorillonite with 2.12% Pd in suspension

0.262 nm^3 for TDOA-montmorillonite (100% exchange). The data clearly show that the volumes available for the nanoparticle formation are significantly different for HDP- and TDOA montmorillonite in THF.

When a calculated amount of Pd(OAc)$_2$ is added to their dispersions (Pd1: 0.1 mmol/g; Pd2: 0.15 mmol/g; Pd3: 0.2 mmol/g) and reduction by ethanol preferentially adsorbed in the interfacial phase (Fig. 1d, 2c), the d_{001} reflection indicates that the formation of Pd$^{\circ}$ particles in the dispersion is associated with an increase of the basal spacing (Fig. 3, 4). It has to be noted that unchanged d_L values in suspension would not necessarily indicate that Pd$^{\circ}$ particles have not been formed in the interlamellar space. As calculated previously, and also shown in Table 1, there is a sufficiently large volume in the swollen state (V_f) with high ethanol content ($x_1{}^s = 0.6$–0.9) to allow the reduction to occur.

When for example, 0.1–0.2 mmol precursor [Pd(OAC)$_2$]/g montmorillonite is added to HDP-montmorillonite suspended in an ethanol-THF mixture with $x_1 = 0.02$, d_L varies between 4.05 and 6.57 nm. The spacing of d_L is 4.39 nm corresponding to the original THF/EtOH mixture and d_L is unchanged by the adsorption of the precursor (Table 1). When the dispersion is dried at 45 °C, d_L is 2.17–2.19 nm and reaches the value measured for dried HDP-montmorillonite. A new

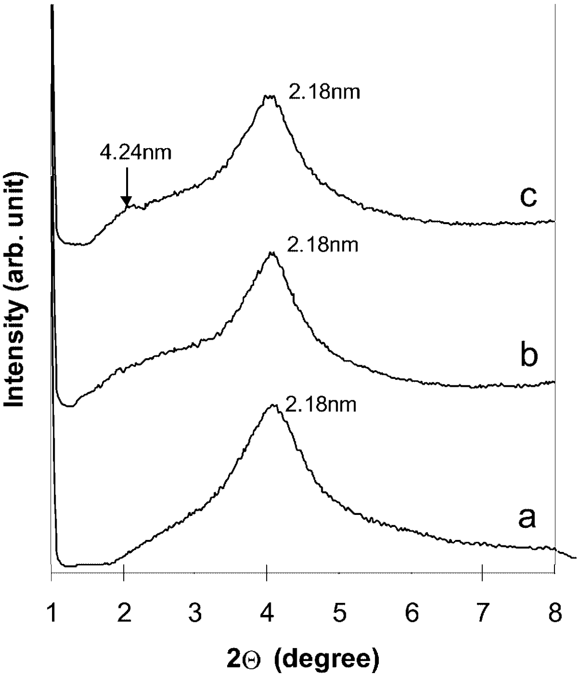

Fig. 4. XRD patterns of (**a**) dried HDP-montmorillonite (**b**) HDP-montmorillonite with 1.6% Pd after drying (**c**) HDP-montmorillonite with 2.12% Pd after drying

Table 1. Basal spacings of hydrophobized montmorillonites (d_L in nm)

Hydrophobized montmorillomte samples		HDP-montm.	TDOA-montm. (50%)	TDOA-montm. (100%)
calc.	d_L, dry	1.88	2.8	2.8
	d_L (I)	2.28	–	–
	d_L (II)	3.61	4.36	4.36
experimantal	d_L, dry	1.87	2.91	3.12
	d_L in THF	3.98	3.4	4.13
	d_L in EtOH	3.35	3.35	3.33
	dt in EtOH/THF	4.39	3.79	3.87
	d_L Pd1, dry	2.18	2.9	3.14
	d_L Pd2, dry	2.18	2.89	3.12
	d_L Pd3,dry	4.24; 2.18	2.89	3.12
	d_L Pd1, in dispersion	4.05	3.6	3.64
	d_L Pd2, in dispersion	4.75	3.65	3.7
	d_L Pd3, in dispersion	6.57; 4.12	3.06	3.73

d_L (I) partially expanded state, d_L (II) totally expanded state
Pd1–1.06w/w% metal content, Pd2–1.6w/w% metal content, Pd3–2.12w/w% metal content

reflection at a basal spacing of 6.57 nm appears in the diffractogram of the sample with the highest metal content (2.12% Pd), in suspension, which decreases to 4.24 nm after drying. In the case of samples with lower metal content, this new peak probably coincides with the first order basal reflection of HDP-montmorillonite, as indicated by the broadening of the peaks (Fig. 4). The calculated interlamellar distance is $d = d_L – 0.96 =$ 3.28 nm and is characteristic of the thickness of the incorporated Pd particles.

The basal spacing of TDOA-montmorillonite (50% c.e.c.) in the THF-ethanol mixture is 3.5–3.8 nm. The formation of Pd^{o} particles between the alkyl chains decreases the basal spacing by about 0.2 nm relative to the value in THF, because the interlamellar swelling is decreased by the reducing agent ethanol. After drying, $d_L = 2.9$ nm is measured, in good agreement with the basal spacing of the dry derivative. This leads to the conclusion that, as a result of drying, Pd^{o} nanoparticles are driven out of the interlamellar space and adhere to the external surface. Thus, the XRD data do not give information on the success of synthesis: it can only be verified by TEM (see below). Similar results are obtained with TDOA-montmorillonite (100% exchange). The basal spacing in the THF-ethanol mixture – when Pd^{o} particles are also present in the course of reduction – varies between 3.64 and 3.73 nm (Fig. 5). After drying, it corresponds to the spacing of the original TDOA-montmorillonite ($d_L = 3.12$–3.14 nm) (Fig. 6). Thus, it is probable that both organophilic montmorillonite supports act as templates for the synthesis as the Pd particles are formed in the interlamellar space, but are found on the external surfaces after removal of the solvent (Fig. 2c, 6b). The primary reason for the displacement of the Pd^{o} nanoparticles from the interlamellar space is that, due to contraction at very high alkyl chain densities (there are four alkyl chains per ion exchange site), no empty "holes" or "dead spaces" remain within the organophilized mineral in which Pd^{o} nanoparticles could be withheld.

The samples were also examined by TEM. One of the samples prepared on HDP-montmorillonite (Pd content 1.06%) is shown in Fig. 7. The average particle size is $d = 2.42$ nm and the surface coverage by Pd^{o} is relatively high, suggesting that particles are present on both the internal and external surfaces of the support. The size distribution of Pd^{o} is nearly monodisperse, varying between 1 nm and 4 nm. The average particle diameter in TDOA-montmorillonite (50% exchange, Pd = 2.12%) is

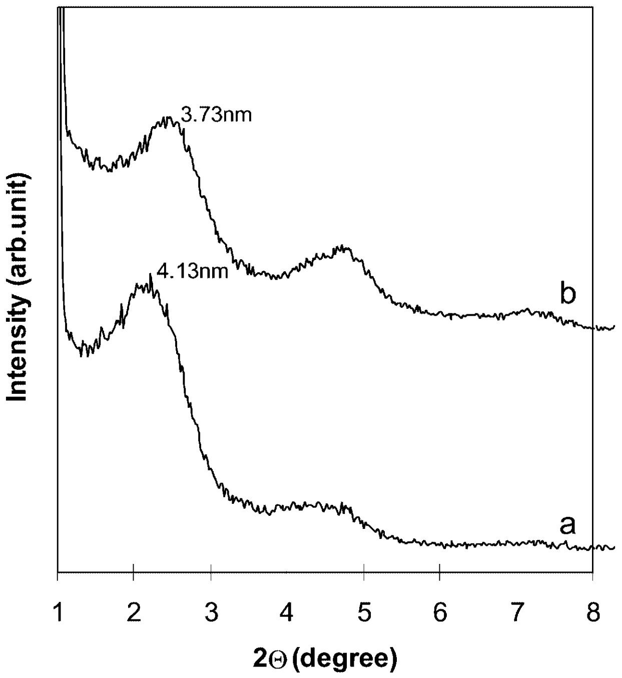

Fig. 5. XRD patterns of (**a**) TDOA-montmorillonite swollen in THF (**b**) TDOA-montmorillonite (100% exchange, 2.12% Pd) in suspension

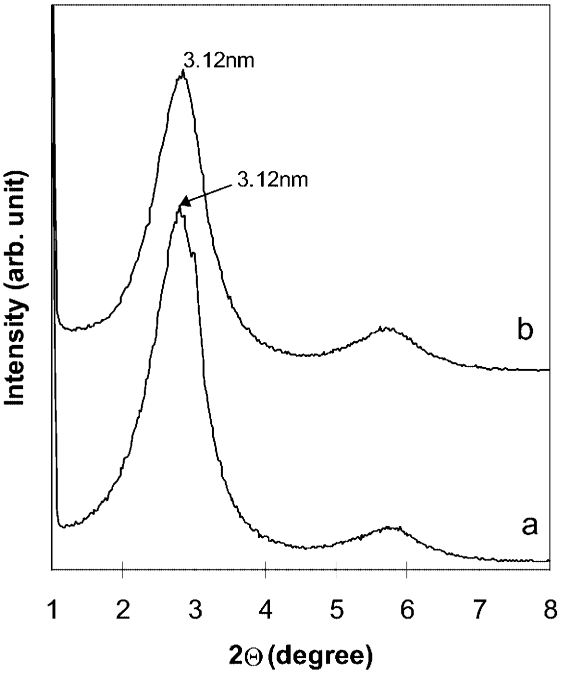

Fig. 6. XRD patterns of (a) dried TDOA-montmorillonite (b) TDOA-montmorillonite (100% exchange, 2.12% Pd) after drying

$d = 3.38$ nm (Fig. 8.) and in TDOA-montmorillonite (100% exchange), $d = 2.96$ nm. Thus, higher interlamellar surfactant content decreased the particle size. The surface density of Pd° particles is lower, indicating that they are indeed present only on the external surfaces of the support. The particle size was also affected by the concentration of the Pd^{2+} precursor. Analysis of TEM pictures of HDP-montmorillonite revealed that d varies between 2 and 5 nm for the concentration range 0.1–0.2 mmol $Pd(OAc)_2$/g organophilic montmorillonite.

Conclusions

The surface and interlamellar volume of hydrophobized clay minerals represent excellent sites for the preparation of metallic palladium nanoparticles in organic medium. A significant portion of Pd° prepared on HDP-montmorillonite is retained between the silicate layers. Calculations from XRD data indicate that there is enough free interlamellar space for formation of the particles. Pd° nanocolloids can also be prepared on montmorillonite hydrophobized with tetraalkylammonium ions. Their size is smaller that that of the Pd° particles prepared on HDP-montmorillonite. As the

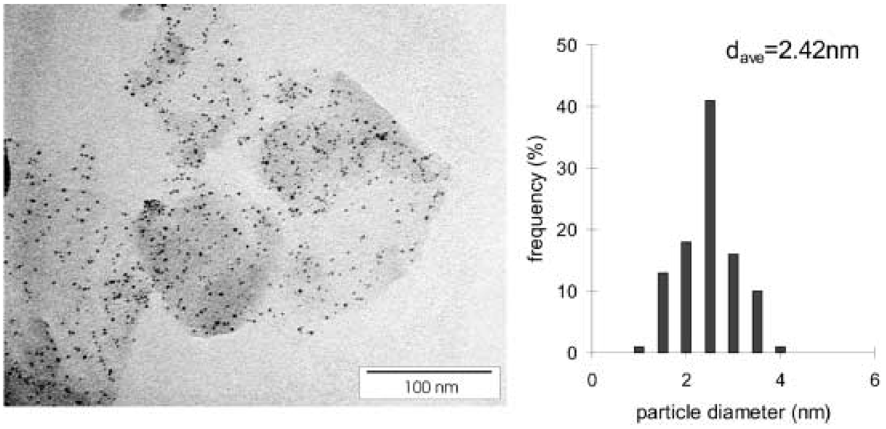

Fig. 7. TEM image and particle size distribution Pd^0 nanoparticles (1.06%Pd) stabilized by HDP-montmorillonite

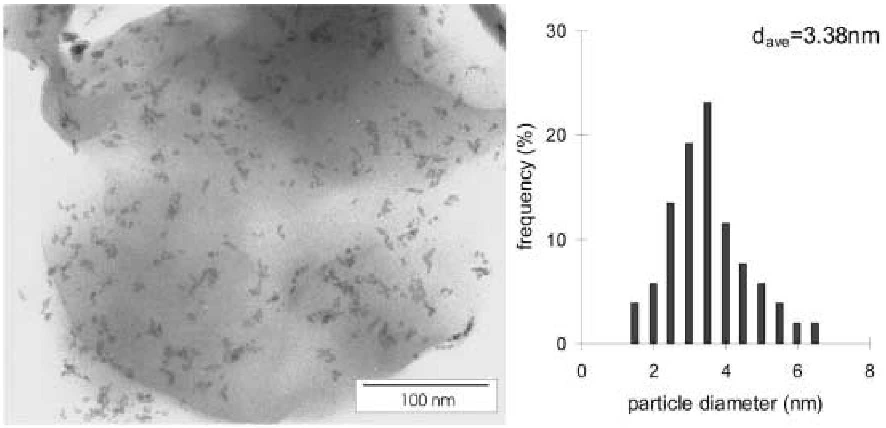

Fig. 8. TEM image and particle size distribution Pd^0 nanoparticles (2.12%Pd) stabilized by TDOA-montmorillonite (50% exchange)

surface density of the alkyl chains is four times higher than in HDP-montmorillonite, Pd^o nanoparticles during drying migrate from the interlamellar space to the external surface. Also, in this case, the hydrophobic montmorillonite acts as a template for the size-controlled Pd^o synthesis.

References

1. Reetz MT, Helbig W, Quasier SA (1996) In: Fürstner A (ed) Active metals preparation, characterization, applications. VCH, Weinheim
2. Schmid G (1992) Chem Rev 92:1709
3. Kotov NA, Meldrum FC, Fendler JH, Tombácz E, Dékány I (1994) Langmuir 10:3797
4. Kotov NA, Dékány I, Fendler JH (1995) J Phys Chem 99:13065
5. Esumi K, Itakura T, Torigoe K (1994) Coll Surf A 82:111
6. Esumi K, Suzuki A, Aihara N, Usui K, Toringoe K (1998) Langmuir 14:3157
7. Mayer ABR, Antonietti M (1998) Coll Polym Sci 276:769
8. Temer SA, Zhong LW, Travis CG, Henglein A, Elsayed A (1996) Science 272:1924
9. Teranishi T, Miyake M (1998) Chem Mater 10:594
10. Toshima N, Harada M, Yonezawa T, Kushihashi K, Asakura K (1991) J Phys Chem 95:7448
11. Bönnemann H, Brijoux W, Brinkmann R, Fretzen R, Joussen T, Köppler R, Korall B, Neiteler P, Richter J (1994) J Mol Catal 86:129
12. Berkovich Y, Garti N (1997) Coll Surf A 128:91
13. Liz-Marzán LM, Lado-Tourino I (1996) Langmuir 12:3585
14. Torigoe K, Esumi K (1992) Langmuir 8:59
15. Yonezawa T, Timinaga T, Toshima N (1995) Langmuir 12:4601
16. Toshima N, Takahashi T (1992) Bull Chem Soc Jpn 65:400
17. Király Z, Veisz B, Mastalir Á, Rázga Zs, Dékány I (1999) Chem Comm 1925
18. Tanori J, Duxin N, Petit C, Lisiecki I, Veillet P, Pileni MP (1995) Coll Polym Sci 273:886
19. Dékány I, Turi L, Tombácz E, Fendler JH (1995) Langmuir 11:2285
20. Dékány I, Nagy L, Turi L, Király Z, Kotov NA, Fendler JH (1996) Langmuir 12(15):3709
21. Dékány I, Fendler JH (1996) In: Pelizetti E (ed), Fine particles. Science and technology. From micro to nanoparticles. NATO ASI Series. Kluwer, p 443
22. Dékány I, Turi L, Szücs A, Király Z (1998) Coll Surf A 141:405
23. Kotov NA, Putyera K, Fendler JH, Tombácz E, Dékány I (1993) Coll Surf A 71:317
24. Mastalir Á, Túri L, Király Z, Dékány I, Bartók M (1998) Mol Cryst Liq Cryst 311:333
25. Aihara N, Torigoe K, Esumi K (1998) Langmuir 14:4945
26. Király Z, Dékány I, Mastalir Á, Bartók M (1996) J Catal 161:401
27. Szücs A, Király Z, Berger F, Dékány I (1998) Coll Surf A 139:109
28. Bartram F (1967) In: Kaelble EF (ed) Crystallite-size determination from line broadening and spotty patterns. Handbook of X-rays. McGraw-Hill, N.Y, chap 17
29. Lagaly G, Stange H, Weiss A (1972) In: Serratosa JM (ed) Proc Int Clay Conference. Madrid, p 693
30. Lagaly G, Weiss A (1971) Angew Chem 83:580
31. Dékany I, Szántó F, Lagaly G, Weiss A (1985) Ber Bunsen Ges Phys Chem 89:62
32. Dékany I, Szántó F, Nagy LG (1985) J Colloid Interface Sci 103:321
33. Dékany I, Szántó F, Nagy LG (1986) J Colloid Interface Sci 109:376